

In an Uncertain World: Distributed Optimization in MIMO Systems with Imperfect Information

Panayotis Mertikopoulos, *Member, IEEE*, and Aris L. Moustakas, *Senior Member, IEEE*

Abstract

In this paper, we introduce a distributed algorithm that optimizes the Gaussian signal covariance matrices of multi-antenna users transmitting to a common multi-antenna receiver under imperfect and possibly delayed channel state information. The algorithm is based on an extension of exponential learning techniques to a semidefinite setting and it requires the same information as distributed water-filling methods. Unlike water-filling however, the proposed matrix exponential learning (MXL) algorithm converges to the system's optimum signal covariance profile under very mild conditions on the channel uncertainty statistics; moreover, the algorithm retains its convergence properties even in the presence of user update asynchronicities, random delays and/or ergodically changing channel conditions. In particular, by properly tuning the algorithm's learning rate (or step size), the algorithm converges within a few iterations, even for large numbers of users and/or antennas per user. Our theoretical analysis is complemented by numerical simulations which illustrate the algorithm's robustness and scalability in realistic network conditions.

Index Terms

Imperfect CSI; matrix exponential learning; MIMO; signal covariance optimization; stochastic approximation.

I. INTRODUCTION

Following the seminal prediction that the use of multiple antennas in signal transmission and reception can lead to substantial performance gains [1, 2], multiple-input and multiple-output (MIMO) technologies have become an integral component of state-of-the-art wireless communication protocols (such as 3G LTE, 4G, HSPA+ and WiMax to name but a few). To capitalize on these gains, the emerging massive MIMO paradigm, a contending technology for 5G networks, “goes large” by scaling up existing multiple-antenna transceivers through the use of inexpensive service antennas and time-division duplexing (TDD) in order to focus energy into ever smaller regions of space [3–5]. In so doing, massive MIMO arrays can increase throughput by a factor of $10\times$ (or more), bring about significant latency reductions over the air interface, and greatly improve the system's robustness to ambient noise [5, 6].

This research was supported in part by the European Commission in the framework of the FP7 Network of Excellence in Wireless Communications NEWCOM# (contract no. 318306), and by the French National Research Agency projects NETLEARN (ANR-13-INFR-004) and GAGA (ANR-13-JS01-0004-01). Part of this work was presented in ISIT 2012 and ISIT 2014 [11, 12].

P. Mertikopoulos is with the French National Center for Scientific Research (CNRS) and the Laboratoire d'Informatique de Grenoble, Grenoble, France; A. L. Moustakas is with the Physics Department, University of Athens, Greece and Supélec, Gif-sur-Yvette, France, supported by the Digiteo Senior Chair "ASAPGONE".

Nevertheless, when coupled with the projected network densification (e.g. due to the massive deployment of small cells), the resulting antenna density is expected to create increased interference which will have to be mitigated through spatial focusing. To that end, it is crucial to optimize the input signal distribution of each user, especially in the moderate signal-to-interference-and-noise ratio (SINR) regime: in this way, wireless receivers can achieve higher transmission rates with the same power, thus increasing spatial spectrum reuse and improving their radiated energy efficiency and overall quality of experience (QoE).

This optimization is typically achieved via water-filling (WF) methods [7–9] that rely on the transmitters having access to accurate channel state information (CSI), including their individual transfer matrices and the multi-user interference-plus-noise (MUI) that they are facing at the receiver. One way to collect the required CSI is to have the base station (BS) emit reverse-link pilot waveforms that allow each terminal to estimate the corresponding channel responses over a given frequency band. However, given that the number of responses that must be estimated at each terminal is proportional to the number of antennas at the BS, massive MIMO systems may require up to a hundred times more pilots than conventional MIMO systems [4]; as such, one of the most popular solutions is to operate in TDD mode and rely on uplink-downlink reciprocity for the exchange of CSI pilot feedback [5].

In this context, a major challenge occurs when transmitters are required to optimize their input signal covariance matrices in the presence of imperfect and/or delayed CSI – e.g. due to the vastly increased impact of pilot contamination in massive MIMO systems [3, 10]. In the absence of perfect channel state information at the transmitter (CSIT), the convergence of WF methods is no longer guaranteed because the algorithms’ fixed point can be significantly perturbed by erroneous (or obsolete) CSI. As a result, the efficient deployment of massive MIMO systems calls for flexible and robust optimization algorithms that are capable of dealing with feedback uncertainty originating from temporal fading, lack of adaptation synchronicity, measurement errors due to noise and pilot contamination, etc.

In this paper, we propose a distributed optimization algorithm based on the method of matrix exponential learning (MXL) that was recently introduced by the authors of [11, 12]. Essentially, rather than updating their signal covariance matrices, transmitters update the logarithm of these matrices based on (possibly imperfect) measurements of a matrix analogue of the transmitter’s SINR. The benefit of updating the logarithm of a user’s covariance matrix is that the algorithm’s updates only need to be Hermitian (and not necessarily positive-definite), so it is much easier to respect the problem’s semidefiniteness constraints. Furthermore, in contrast to WF methods, the proposed algorithm proceeds by *aggregating* CSI feedback over time: in this way, measurement errors, noise and asynchronicities effectively vanish in the long run thanks to the law of large numbers for martingales. In particular, the proposed algorithm has the following desirable attributes:

- 1) It is *distributed*: user updates are based on local information and channel measurements.
- 2) It is *robust*: measurements and observations may be subject to random errors and noise.
- 3) It is *stateless*: users do not need to know the state (or topology) of the system.
- 4) It is *reinforcing*: each user tends to increase his own rate.
- 5) It is *decentralized*: user updates need not be synchronized or otherwise coordinated.

A good paradigm to test the performance and convergence properties of the proposed algorithm is the widely studied vector Gaussian multiple access channel (MAC) [8]. This channel model is the MIMO equivalent of the parallel multiple access channel (PMAC) and consists of several (and mutually independent) MIMO transceivers that are linked to a common multi-antenna receiver. In this framework, assuming perfect CSIT, it is well known that iterative water-filling (IWF) converges to the system’s optimum transmit profile [8], but the algorithm’s convergence speed decreases proportionally with the number of transmitting users. On the other hand, simultaneous water-filling (SWF) is much faster, but it may fail to converge altogether: as was shown in [13], the sufficient conditions that guarantee the convergence of SWF methods may fail to hold even in simple 2×2 PMAC systems; To make matters worse, this situation is exacerbated in the case of imperfect CSI where even the convergence of IWF is no longer guaranteed; by contrast, the proposed MXL algorithm converges rapidly to the system’s optimum transmit profile (even for large numbers of users and/or antennas per user), and it remains convergent irrespective of the magnitude of the measurement noise.

Our theoretical analysis relies on the powerful stochastic approximation methods of [14, 15] and the matrix regularization machinery of [16, 17]. Specifically, we first establish the algorithm’s convergence in a continuous-time setting, and we then use the ODE method of stochastic approximation [14] and the theory of concentration inequalities for martingales [18, 19] to show that this convergence is retained in a discrete-time setting – even under noisy and delayed/asynchronous updates.¹ The algorithm’s main tunable parameter is its step-size which controls the rate at which users learn: picking larger step sizes accelerates the algorithm, but this acceleration comes at the expense of accuracy (a crucial trade-off in the presence of noise). Still, if the error process has finite p -th moments for some $p \geq 20$, convergence is guaranteed as long as the algorithm’s step-size γ_n satisfies $\sum_n \gamma_n^{1+p/2} < \infty$; in practice, the central limit theorem guarantees that estimators of Gaussian variables have finite moments of every order, so the algorithm’s step-size can be taken nearly constant, guaranteeing in this way relatively rapid convergence even in very noisy environments. In addition, we show that, under mild conditions on the moments of the error process, the tail behavior of the deviations is Gaussian – i.e. it is sharply concentrated around its mean.

Paper outline and summary of results

After introducing our system model in the next section, we derive the proposed matrix exponential learning algorithm in Section III-A (cf. Algorithm 1); in the same section, we also state our main convergence result in the presence of measurement noise and errors (Theorem 1). Since one of the main goals of this paper is to illustrate the convergence properties of MXL in the presence of various stochastic impediments, Section III-B provides a concrete example of feedback matrix estimation, while Section III-C extends the convergence results of Section III-A to the case of asynchronous user updates (Theorem 2). Section III-D describes the evolution of the eigenvalues and eigenvectors of the users’ signal covariance matrices (Theorem 3), while Section IV extends our results further to the case of fast-

¹For a related continuous-to-discrete descent, see the recent paper [20] on unilateral online optimization in dynamically varying cognitive radio systems.

fading channels (Theorem 4). Finally, our theoretical analysis is validated and supplemented by numerical simulations in Section V.

To streamline the flow of the paper, proofs and technical details have been delegated to a series of appendices at the end.

II. SYSTEM MODEL

Consider a Gaussian vector multiple access channel (MAC) where a finite set of wireless users $k \in \mathcal{K} \equiv \{1, \dots, K\}$ transmit simultaneously over a common channel to a base receiver with N antennas. If the k -th transmitter is equipped with M_k transmit antennas, we get the familiar signal model

$$\mathbf{y} = \sum_{k=1}^K \mathbf{H}_k \mathbf{x}_k + \mathbf{z}, \quad (1)$$

where:

- 1) $\mathbf{x}_k \in \mathbb{C}^{M_k}$ is the message transmitted by user $k \in \mathcal{K}$.
- 2) $\mathbf{y} \in \mathbb{C}^N$ denotes the aggregate signal at the receiver.
- 3) $\mathbf{H}_k \in \mathbb{C}^{N \times M_k}$ is the $N \times M_k$ channel matrix of user k .
- 4) $\mathbf{z} \in \mathbb{C}^N$ is the ambient noise in the channel, including thermal, atmospheric and other peripheral interference effects (and modeled for simplicity as a zero-mean, complex Gaussian vector with unit covariance).²

In this context, the average transmit power of user k is simply

$$p_k = \mathbb{E} [||\mathbf{x}_k||^2] = \text{tr}(\mathbf{Q}_k), \quad (2)$$

where \mathbf{Q}_k denotes the user's signal covariance matrix:

$$\mathbf{Q}_k = \mathbb{E} [\mathbf{x}_k \mathbf{x}_k^\dagger], \quad (3)$$

and the expectation is taken over the Gaussian codebook of user k . Hence, assuming that each user's maximum transmit power is finite, we obtain the feasibility constraints:

$$\mathbf{Q}_k \succeq 0 \quad \text{and} \quad \text{tr}(\mathbf{Q}_k) \leq P_k, \quad (4)$$

where $P_k > 0$ denotes the maximum transmit power of user k .

The first part of our analysis focuses on *static channels*, i.e. the channel matrices \mathbf{H}_k will be assumed to remain constant (or nearly constant) throughout the transmission horizon (fast-fading channels will be treated in Section IV). In this case, assuming single user decoding (SUD) at the receiver (i.e. interference by all other users is treated as additive colored noise), each user's achievable transmission rate will be given by the familiar expression [2]:

$$R_k(\mathbf{Q}) = \log \det (\mathbf{W}_{-k} + \mathbf{H}_k \mathbf{Q}_k \mathbf{H}_k^\dagger) - \log \det (\mathbf{W}_{-k}), \quad (5)$$

²Obviously, depending on the structure and statistical properties of the channel matrices \mathbf{H}_k , the signal model (1) could be applied to a wide variety of telecommunications systems, ranging from digital subscriber line (DSL) uplink networks with Toeplitz circulant \mathbf{H}_k to code division multiple access (CDMA) and/or frequency division multiple access (FDMA) radio networks [21]. For concreteness however, we will interpret (1) as an ad hoc multi-user MIMO multiple access channel with \mathbf{H}_k representing the channel of each link.

where $\mathbf{Q} = (\mathbf{Q}_1, \dots, \mathbf{Q}_K)$ and

$$\mathbf{W}_{-k} = \mathbf{I} + \sum_{\ell \neq k} \mathbf{H}_\ell \mathbf{Q}_\ell \mathbf{H}_\ell^\dagger \quad (6)$$

represents the multi-user interference-plus-noise (MUI) covariance matrix of user k . Thus, given that each user needs to saturate his power constraints in order to maximize his individual rate, we will say that a transmit profile $\mathbf{Q}^* = (\mathbf{Q}_1^*, \dots, \mathbf{Q}_K^*)$ is at *Nash equilibrium* when no user can unilaterally improve his individual achievable rate R_k , i.e.

$$R_k(\mathbf{Q}^*) \geq R_k(\mathbf{Q}_k; \mathbf{Q}_{-k}^*) \quad \text{for all } \mathbf{Q}_k \in \mathcal{X}_k, k \in \mathcal{K}, \quad (\text{NE})$$

where $(\mathbf{Q}_k; \mathbf{Q}_{-k}^*)$ is shorthand for $(\mathbf{Q}_1^*, \dots, \mathbf{Q}_k, \dots, \mathbf{Q}_K^*)$ and

$$\mathcal{X}_k = \{\mathbf{Q}_k \in \mathbb{C}^{M_k \times M_k} : \mathbf{Q}_k \succeq 0, \text{tr}(\mathbf{Q}_k) = P_k\} \quad (7)$$

denotes the (compact, convex) set of feasible signal covariance matrices for user k .³

Dually to the above, if the receiver employs successive interference cancellation (SIC) techniques to decode the received messages, the users' achievable sum rate will be [8]:

$$R(\mathbf{Q}) = \log \det \left(\mathbf{I} + \sum_k \mathbf{H}_k \mathbf{Q}_k \mathbf{H}_k^\dagger \right). \quad (8)$$

In this way, we obtain the sum rate maximization problem:

$$\begin{aligned} & \text{maximize} && R(\mathbf{Q}), \\ & \text{subject to} && \mathbf{Q}_k \in \mathcal{X}_k, k = 1, \dots, K. \end{aligned} \quad (\text{RM})$$

Importantly, as can be easily checked, the users' sum rate (8) is a *potential function* for the game defined by (5) in the sense that

$$R_k(\mathbf{Q}_k; \mathbf{Q}_{-k}) - R_k(\mathbf{Q}'_k; \mathbf{Q}_{-k}) = R(\mathbf{Q}_k; \mathbf{Q}_{-k}) - R(\mathbf{Q}'_k; \mathbf{Q}_{-k}). \quad (9)$$

Hence, with R concave, it follows that the solutions of the Nash equilibrium problem (NE) coincide with the solutions of (RM); put differently, *optimizing the users' achievable sum rate (8) under SIC is equivalent to equilibrating the users' individual transmission rates (5) under SUD*.

For concreteness, in the rest of this paper, we will focus on the sum rate maximization problem (RM); however, owing to the above observation, our results will obviously apply to the unilateral equilibration problem (NE) as well.

III. LEARNING WITH IMPERFECT AND DELAYED INFORMATION

The sum rate maximization problem (RM) is traditionally solved by water-filling (WF) methods [7], either iterative [8, 22] or simultaneous [23]. More precisely, transmitters are typically assumed to have perfect knowledge of the channel matrices \mathbf{H}_k and the aggregate signal-plus-noise covariance matrix

$$\mathbf{W} = \mathbb{E}[\mathbf{y}\mathbf{y}^\dagger] = \mathbf{I} + \sum_\ell \mathbf{H}_\ell \mathbf{Q}_\ell \mathbf{H}_\ell^\dagger, \quad (10)$$

³Under an energy-aware objective, users would not need to saturate their power constraints, but such considerations lie beyond the scope of this paper.

which is in turn used to calculate the MUI covariance matrices $\mathbf{W}_{-k} = \mathbf{W} - \mathbf{H}_k \mathbf{Q}_k \mathbf{H}_k^\dagger$ and “water-fill” the effective channel matrices $\tilde{\mathbf{H}}_k = \mathbf{W}_{-k}^{-1/2} \mathbf{H}_k$ at the transmitter [8]. At a multi-user level, this water-filling process could take place either iteratively (with users updating their covariance matrices in a round robin fashion) [8] or simultaneously (with all users updating at once) [23]: the former updating scheme converges always (but slowly for large numbers of users) [8], whereas the latter is much faster [23] but may occasionally fail to converge, even in simple, 2-user parallel multiple access channels [13].

An added complication in the use of WF methods is that they rely on perfect channel state information at the transmitter (CSIT) and accurate measurements of \mathbf{W} at the receiver (who can broadcast this information via a dedicated radio channel or as part of the TDD downlink phase). When such measurements are not available, it is not known whether WF methods converge; on that account, our goal in this section will be to describe a distributed learning method that allows users to attain the system’s sum capacity in a distributed way, using only imperfect (and possibly delayed) information.

A. Matrix exponential learning

Instead of relying on fixed-point methods, our approach will rely on tracking the direction of steepest ascent of the system’s sum rate in a dual, unconstrained space, and then map the result back to the problem’s feasible space via matrix exponentiation. Formally, assuming for the moment perfect CSIT, we will consider the MXL scheme:

$$\begin{aligned} \mathbf{Y}_k(n+1) &= \mathbf{Y}_k(n) + \gamma_n \mathbf{V}_k(\mathbf{Q}(n)), \\ \mathbf{Q}_k(n+1) &= P_k \frac{\exp(\mathbf{Y}_k(n+1))}{\text{tr}[\exp(\mathbf{Y}_k(n+1))]}, \end{aligned} \tag{MXL}$$

where:

- 1) $\mathbf{V}_k \equiv \mathbf{V}_k(\mathbf{Q})$ denotes the (matrix) derivative of the system’s sum rate with respect to each user’s covariance matrix:

$$\mathbf{V}_k(\mathbf{Q}) \equiv \nabla_{\mathbf{Q}_k} R = \nabla_{\mathbf{Q}_k} R_k = \mathbf{H}_k^\dagger \mathbf{W}^{-1} \mathbf{H}_k \tag{11}$$

- 2) \mathbf{Y}_k is an auxiliary “scoring” matrix which tracks the direction of steepest sum rate ascent.
- 3) γ_n is a decreasing step-size sequence (typically, $\gamma_n = 1/n$).

Remark 1. Given that $R(\mathbf{Q})$ is real-valued, \mathbf{V}_k and \mathbf{Y}_k are automatically Hermitian, so the matrix exponential $\exp(\mathbf{Y}_k)$ is positive-definite, as required; the trace normalization in (MXL) then ensures that $\mathbf{Q}_k(n)$ satisfies the feasibility constraints (7) of (RM) for all $n \geq 1$. In this way, (MXL) can be seen as a two-stage, “primal-dual” gradient method [24] which reinforces the spatial directions that lead to higher sum rates by allocating more power to the corresponding eigen-directions of the users’ covariance matrices.

To account for imperfect CSIT and noisy measurements at the receiver, we will assume that the gradient matrices \mathbf{V} of (11) are only known up to a noisy estimate $\hat{\mathbf{V}}$. In particular, we envision the following sequence of events:

- 1) At every update period $n = 1, 2, \dots$, each user $k \in \mathcal{K}$ gets an estimate $\hat{\mathbf{V}}_k(n)$ of the true gradient matrix $\mathbf{V}_k(\mathbf{Q}(n))$.
- 2) Users update their signal covariance matrices according to (MXL) and the process repeats.

More concretely, this recurring process may be encoded in algorithmic form as follows:

Algorithm 1 Matrix Exponential Learning (MXL).

 Parameter: decreasing step-size sequence γ_n

 Initialize: $n \leftarrow 0$; $\mathbf{Y}_k \leftarrow \mathbf{0}$; $\mathbf{Q}_k \leftarrow \frac{P_k}{M_k} \cdot \mathbf{I}$
Repeat
 $n \leftarrow n + 1$;
foreach user $k \in \mathcal{K}$ **do**
 receive estimate $\hat{\mathbf{V}}_k$ of $\mathbf{V}_k = \mathbf{H}_k^\dagger \mathbf{W}^{-1} \mathbf{H}_k$;

 update score matrix: $\mathbf{Y}_k \leftarrow \mathbf{Y}_k + \gamma_n \hat{\mathbf{V}}_k$;

 set covariance matrix: $\mathbf{Q}_k \leftarrow P_k \cdot \exp(\mathbf{Y}_k) / \text{tr}[\exp(\mathbf{Y}_k)]$;

until termination criterion is reached.

The MXL algorithm above will be the main focus of our paper, so a few remarks are in order:

a) *Implementation*: From an implementation point of view, MXL has the following desirable properties:

(P1) *Distributedness*: users have the same information requirements as in distributed water-filling [8, 22, 23].

(P2) *Robustness*: the algorithm does not assume perfect CSIT or precise signal measurements at the receiver.

(P3) *Statelessness*: users do not need to know the state of the system (e.g. its topology).

(P4) *Reinforcement*: users reinforce the transmit directions that lead to higher transmission rates.

b) *Assumptions on the measurement errors*: Throughout this paper, we will work with the following statistical hypotheses for the noise process $\mathbf{Z}_k(n) = \hat{\mathbf{V}}_k(n) - \mathbf{V}_k(\mathbf{Q}(n))$:

(H1) *Unbiasedness*:

$$\mathbb{E}[\mathbf{Z}(n+1) \mid \mathbf{Q}(n)] = \mathbf{0}. \quad (\text{H1})$$

(H2) *Finite mean squared error (MSE)*:

$$\mathbb{E}[\|\mathbf{Z}(n+1)\|^2 \mid \mathbf{Q}(n)] \leq \sigma^2 \quad \text{for some } \sigma > 0. \quad (\text{H2})$$

The statistical hypotheses above allow us to account for a very wide range of error processes: in particular, we will *not* be assuming independent and identically distributed (i.i.d.) errors, or even errors that are a.s. bounded.⁴ In fact, Hypotheses (H1) and (H2) simply amount to asking that the gradient estimate $\hat{\mathbf{V}}$ be unbiased and bounded in mean square:

$$\mathbb{E}[\|\hat{\mathbf{V}}_k(n+1)\|^2 \mid \mathbf{Q}(n)] \leq V_k^2 \quad \text{for some } V_k > 0, \quad (12)$$

and our convergence results will be stated with only this mild requirement in mind.

That being said, we obtain even sharper results in some cases under the additional hypothesis:

(H3) *Conditionally symmetric error distributions*: the law of $\mathbf{Z}(n+1)$ given $\mathbf{Q}(n)$ is symmetric.

Hypothesis (H3) also applies to the vast majority of centered processes (uniform, Gaussian, Lévy α -stable, Laplace, etc.) and we will use it to further refine our convergence results.

⁴This observation is crucial in the context of wireless networks because measurement errors are typically correlated with the state of the system.

c) *The estimation process:* As stated, Algorithm 1 does not detail how the system's users can obtain an unbiased estimate $\hat{\mathbf{V}}_k$ of \mathbf{V}_k from individual CSI observations and measurements of the received signal covariance matrix \mathbf{W} . To simplify our presentation, we will state our convergence results below under the assumption that there is an oracle-like mechanism that returns such estimates to the users on request; the construction of such a mechanism will then be detailed in Section III-B.

Remark. We should also note here that if the gradient estimates $\hat{\mathbf{V}}_k$ are not Hermitian, the score matrices $\hat{\mathbf{Y}}$ will not be Hermitian either so the users' covariance matrices may fail to be positive-definite. To avoid such complications, it suffices to take $[\hat{\mathbf{V}} + \hat{\mathbf{V}}^\dagger]/2$ of $\hat{\mathbf{V}}$ as an estimator for \mathbf{V} ; for simplicity, we will tacitly assume that this hermitization step has already taken place if necessary.

d) *Complexity per iteration:* From a computational standpoint, it is easy to see that the complexity of each iteration of Algorithm 1 is polynomial (with a low degree) in the number of transmit and receive antennas (for calculations at the transmitter and receiver side respectively). Specifically, the complexity of the required matrix inversion and exponentiation steps is $O(N^\omega)$ and $O(M_k^\omega)$ respectively, where the exponent ω is as low as 2.373 if the processing units employ fast Coppersmith–Winograd methods for matrix multiplication [25].⁵ The Hermitian structure of \mathbf{W} can be exploited to reduce the computational cost of each iteration even further, but such issues lie beyond the scope of this paper; in practice, the number of transmit and receive antennas are physically constrained by the size of the wireless array, so these operations are quite light.

With all this in mind, our main result is as follows:

Theorem 1. *Assume that the MXL algorithm (Alg. 1) is run with nonincreasing step-sizes γ_n such that $\sum_n \gamma_n^2 < \infty$ and noisy measurements $\hat{\mathbf{V}}(n)$ satisfying hypotheses (H1) and (H2). Then, $\mathbf{Q}(n)$ converges almost surely to $\arg \max_{\mathbf{Q}} R(\mathbf{Q})$.*

More generally, let $\bar{R}_n = \sum_{j=1}^n \gamma_j R_j / \sum_{j=1}^n \gamma_j$ denote the time average of the users' sum rate with respect to an arbitrary nonincreasing step-size sequence γ_n . Then:

$$i) \quad \mathbb{E}[\bar{R}_n] \geq R_{\max} - \varepsilon_n, \quad (13)$$

$$ii) \quad \mathbb{P}(R_{\max} - \bar{R}_n \geq \varepsilon_n + z) = O\left(\sigma^2 z^{-2} t_n^{-2} \sum_{j=1}^n \gamma_j^2\right) \quad (14)$$

where $R_{\max} = \max_{\mathbf{Q}} R(\mathbf{Q})$ is the system's sum capacity, $t_n = \sum_{j=1}^n \gamma_j$, and

$$\varepsilon_n = t_n^{-1} \left[\sum_{k=1}^K \log M_k + \frac{1}{2} L^2 \sum_{j=1}^n \gamma_j^2 \right], \quad (15)$$

denotes the algorithm's mean performance guarantee at the n -th update period (in the above, M_k is the number of transmit antennas of user k and $L^2 = \sum_{k=1}^K P_k^2 V_k^2$ is a positive constant depending on the users' maximum transmit powers P_k and the mean square V_k^2 of their measurements).

⁵In particular, the complexity of each iteration of Algorithm 1 is that of matrix multiplication.

Finally, if (H3) also holds, the concentration of the algorithm around its mean value at a given iteration is exponential:

$$-\log \mathbb{P}(R_{\max} - \bar{R}_n \geq \varepsilon_n + z) = O\left(t_n^2 z^2 \sigma^{-2} / \sum_{j=1}^n \gamma_j^2\right) \quad (16)$$

Proof: See Appendix B. ■

In what follows, we discuss some important points regarding Theorem 1:

a) *On the choice of γ_n :* The use of a decreasing step-size sequence γ_n in (MXL) might appear counter-intuitive because it implies that new gradients enter the algorithm with *decreasing weights* (after all, intuition suggests that one should put more weight on recent observations rather than older, obsolete ones). However, if the algorithm has reached a near-optimal point, a constant step size might cause it to overshoot and miss its mark: this can be seen clearly from the mean error bound (15) which does not vanish as $n \rightarrow \infty$ for constant step sizes of the form $\gamma_n = \gamma$.

As a rule of thumb, the use of a (large) constant step size speeds up the algorithm but may also lead to unwanted oscillations towards the end because it does not dissipate measurement noise and discretization errors: if the system's users seek to eliminate such phenomena, a decreasing step size should be preferred instead. In fact, to obtain the best of both worlds, we can consider an adaptive schedule where the method's step-size is initially very high (to accelerate the search of the problem's state space), and is then abruptly decreased when oscillations are detected; we test such schedules in Section V.

We should also note here that the requirement $\sum_n \gamma_n^2 < \infty$ for almost sure convergence is tied to the finite MSE hypothesis (H2) and can be relaxed significantly if there are sharper bounds on the central moments of the estimator $\hat{\mathbf{V}}$. For instance, if the error process $\mathbf{Z}(n)$ has finite p -th moments (cf. Hypothesis (H2') below), the analysis of [14] shows that the summability condition $\sum_n \gamma_n^2 < \infty$ can be replaced by the much lighter requirement $\sum_n \gamma_n^{1+p/2} < \infty$ which allows us to use considerably faster step-size sequences.

b) *Convergence rate:* If users employ a constant step-size sequence $\gamma_j = \gamma$ for a number of iterations n that is *fixed in advance* (using “for” instead of “while”), an easy calculation shows that the minimum value of the mean guarantee (15) is attained for $\gamma_j = \gamma = L^{-1} \sqrt{2 \sum_k \log M_k / n}$ and is equal to:⁶

$$\varepsilon_n = L \sqrt{\frac{2 \sum_k \log M_k}{n}}. \quad (17)$$

Put differently, the mean performance guarantee (15) with constant step size falls below $\varepsilon > 0$ in $n = 2L^2 \sum_k \log M_k / \varepsilon^2 = O(K\varepsilon^{-2})$ iterations.

That being said, this guarantee concerns the *empirical average* of the system's sum rate $\bar{R}_n = n^{-1} \sum_j R_j$ and not the users' *instantaneous* sum rate R_n . Empirical averages evolve much slower than actual values and, as we show in Section V, the users' instantaneous sum rate R_n increases much faster and converges to the system's sum capacity within a few iterations (even for very large numbers of users and/or antennas per user).

⁶Note also that \bar{R}_n is then given by the standard expression $\bar{R}_n = n^{-1} \sum_{j=1}^n R_j$.

c) *Large deviations and outage probabilities:* Eq. (14) represents the probability of observing sum rates far below the channel's capacity, so it can be interpreted as a measure of the system's outage probability under (MXL). As such, the tail behavior of (14) shows that MXL hardens considerably around its deterministic limit: even though measurement errors can become arbitrarily large (note that a finite MSE does not imply a.s. bounded errors), the probability of observing sum rates much lower than what is obtainable with perfect gradient measurements decays very fast – exponentially so if (H3) holds. In particular, for large n , the step-size factor $t_n^{-2} \sum_{j=1}^n \gamma_j^2$ which controls the width of non-negligible large deviations (the parameter z) in (14) is of order $\mathcal{O}(1/n)$ for step-size sequences of the form $\gamma_n \propto n^{-a}$, $a \in (0, 1/2)$, and of order $\mathcal{O}(n^{2a-2})$ for $a \in (1/2, 1)$.

Finally, we should also note that the symmetry condition (H3) is not at all necessary to obtain the exponential rate of decay (16). As we show in Appendix B, the same bound is also obtained under the following slight reinforcement of (H2):

(H2') *Subexponential error moment growth:*

$$\mathbb{E} \left[\|\hat{\mathbf{V}}(n+1) - \mathbf{V}(\mathbf{Q}(n+1))\|^p \mid \mathbf{Q}(n) \right] \leq \frac{p!}{2} \sigma^p \quad (\text{H2}')$$

for some $\sigma > 0$ and for all $p \in \mathbb{N}$.

This hypothesis is also satisfied by a wide range of probability distributions (including all distributions with finite support, Gaussian, sub-Gaussian and sub-exponential tails) and it offers a useful alternative to (H3) when the only thing that can be estimated is the errors' raw moments.

d) *Links with matrix regularization:* The proof of Theorem 1 relies on stochastic approximation techniques [14] and a deep connection between matrix exponentiation and the von Neumann quantum entropy. In fact, as we show in the appendix, (MXL) is closely related to the matrix regularization techniques of [16, 17, 20] for online learning and the mirror descent machinery of [24, 26] for (stochastic) convex programming. In particular, the “convergence-in-the-mean” bound (13) is derived in the same way as the corresponding results of [24, 26], but the techniques developed therein do not suffice for the much stronger almost sure convergence result that we present here. An in-depth description of mirror descent methods requires the introduction of considerable technical apparatus from convex analysis and lies beyond the scope of this paper; for a comprehensive account, see instead [24, 26] and references therein.

B. Unbiased gradient estimators

As we mentioned before, the MXL algorithm requires users to have access to unbiased estimates $\hat{\mathbf{V}}_k$ of their individual gradient matrices (11). Our goal in this section will be to describe a process with which the receiver and the transmitters may estimate \mathbf{V} based at each step on possibly imperfect signal and channel measurements – e.g. obtained through the exchange of pilot feedback signals.

The first step will be to estimate the aggregate *signal precision* (inverse covariance) matrix

$$\mathbf{P} = \mathbb{E}[\mathbf{y}\mathbf{y}^\dagger]^{-1} = \mathbf{W}^{-1} = \left(\mathbf{I} + \sum_{\ell} \mathbf{H}_{\ell} \mathbf{Q}_{\ell} \mathbf{H}_{\ell}^\dagger \right)^{-1} \quad (18)$$

by sampling the signal $\mathbf{y} \in \mathbb{C}^N$ at the receiver. To that end, since the channel is Gaussian, an unbiased estimate for the received signal covariance $\mathbf{W} = \mathbb{E}[\mathbf{y}\mathbf{y}^\dagger]$ can be obtained from a systematically unbiased sample $\{\mathbf{y}_s\}_{s=1}^S$ of size S by means of the well-known estimator $\hat{\mathbf{W}} = \frac{1}{S} \sum_{s=1}^S \mathbf{y}_s \mathbf{y}_s^\dagger$.⁷ However, $\hat{\mathbf{W}}^{-1}$ is a *biased* estimate for \mathbf{W}^{-1} , so inverting $\hat{\mathbf{W}}$ directly would introduce a systematic error in $\hat{\mathbf{P}}$. Instead, following [27], we will consider the bias-adjusted precision matrix estimator:

$$\hat{\mathbf{P}} = \frac{S - N - 1}{S} \hat{\mathbf{W}}^{-1}, \quad (19)$$

where N is the number of antennas at the receiver (the dimension of \mathbf{y}) and $\hat{\mathbf{W}} = S^{-1} \sum_{s=1}^S \mathbf{y}_s \mathbf{y}_s^\dagger$ as before.

Consequently, in the absence of perfect channel state information at the transmitter, the transmitters must estimate the individual gradient matrices $\mathbf{V}_k = \mathbf{H}_k^\dagger \mathbf{W}^{-1} \mathbf{H}_k$ from the broadcast of $\hat{\mathbf{P}}$ and using imperfect measurements of their channel matrices \mathbf{H}_k . To that end, if each transmitter takes S independent measurements $\hat{\mathbf{H}}_{k,1}, \dots, \hat{\mathbf{H}}_{k,S}$ of his channel matrix (e.g. via independent pilot sampling), an unbiased Hermitian estimate for \mathbf{V}_k is given by the expression:

$$\hat{\mathbf{V}}_k = \frac{1}{S(S-1)} \sum_{s \neq s'} \hat{\mathbf{H}}_{k,s}^\dagger \hat{\mathbf{P}} \hat{\mathbf{H}}_{k,s'}, \quad (20)$$

where $\hat{\mathbf{P}}$ is the latest estimate of (19) of \mathbf{W}^{-1} that was broadcast by the receiver.⁸ Indeed, given that the sampled channel matrix measurements $\hat{\mathbf{H}}_{k,s}$ are assumed stochastically independent, we readily obtain:

$$\mathbb{E}[\hat{\mathbf{V}}_k] = \frac{1}{S(S-1)} \sum_{s \neq s'} \mathbb{E}[\hat{\mathbf{H}}_{k,s}^\dagger \hat{\mathbf{P}} \hat{\mathbf{H}}_{k,s'}] = \mathbf{H}_k^\dagger \mathbf{W}^{-1} \mathbf{H}_k, \quad (21)$$

i.e. (20) constitutes an unbiased estimator of \mathbf{V} .

The construction above provides an estimator $\hat{\mathbf{V}}$ with $\mathbb{E}[\hat{\mathbf{V}}] = \mathbf{V}$, so Assumption (H1) holds. As for the variance of $\hat{\mathbf{V}}$, (20) can also be used to derive an expression for $\text{Var}(\hat{\mathbf{V}})$ in terms of the moments of $\hat{\mathbf{P}}$ and $\hat{\mathbf{H}}$. Since the system input and noise are assumed Gaussian, the former are all finite (and Gaussian-distributed) so the finite mean square error hypothesis (H2) boils down to measuring \mathbf{H} with finite mean squared error – a requirement which is easy to achieve. In fact, if the sample size S is taken large enough, the central limit theorem guarantees significant control on the variance and higher central moments of $\hat{\mathbf{V}}$, so even the tighter requirements (H2') and (H3) hold.

Remark 2. Under time-division duplexing (TDD) operation, the estimation process above is greatly facilitated because the estimates of each user's channel matrix \mathbf{H}_k can be calculated directly at the transmitter via reverse-link pilots. In the absence of TDD (or in the case where the number of antennas at the receiver is massively large, viz. $N^2 \gg \sum_k M_k^2$), a more efficient solution would be to feed back to each transmitter an unbiased estimate of \mathbf{V}_k that is calculated directly at the receiver.

C. Asynchronous updates and delays

Even though the information requirements of (MXL) are local in nature, the algorithm itself is not fully decentralized because it relies implicitly on a global timer to coordinate the users' update schedule (similarly to IWF and SWF

⁷Since the expected value $\mathbb{E}[\mathbf{y}] = 0$ of \mathbf{y} is known in advance, we do not need to include an $S/(S-1)$ bias correction factor in the estimate of \mathbf{W} .

⁸Obviously, increasing the sample size S decreases the estimator's MSE at the cost of computational complexity.

methods). To overcome this limitation, we examine here a fully decentralized variant of Algorithm 1 where each user updates his signal covariance matrix based on an individual timer and completely independently of other users.

Of course, in this case, the measurements $\hat{\mathbf{V}}_k$ may suffer from delays and asynchronicities, so the update structure of Algorithm 1 must be suitably modified. To that end, let n denote the n -th *overall* update period in the system, let $\mathcal{K}_n \subseteq \mathcal{K}$ denote the subset of users who update at this epoch (typically $|\mathcal{K}_n| = 1$ if users update at random times), and let $d_k(n)$ be the number of periods that have elapsed since the last update of the k -th user. We then obtain the following asynchronous variant of (MXL):

$$\begin{aligned} \mathbf{Y}_k(n+1) &= \mathbf{Y}_k(n) + \gamma_{n_k} \mathbb{1}(k \in \mathcal{K}_n) \cdot \hat{\mathbf{V}}_k(n), \\ \mathbf{Q}_k(n+1) &= P_k \frac{\exp(\mathbf{Y}_k(n+1))}{\text{tr}[\exp(\mathbf{Y}_k(n+1))]}, \end{aligned} \quad (\text{MXL-a})$$

where $n_k = \sum_{j=1}^n \mathbb{1}(k \in \mathcal{K}_j)$ denotes the number of updates that have been performed by user k up to epoch n and $\hat{\mathbf{V}}_k$ is a noisy (and asynchronous) estimate of (11):

$$\hat{\mathbf{V}}_k(n) = \mathbf{H}_k^\dagger \left[\mathbf{I} + \sum_{\ell} \mathbf{H}_\ell \mathbf{Q}_\ell(n - d_\ell(n)) \mathbf{H}_\ell^\dagger \right]^{-1} \mathbf{H}_k + \mathbf{Z}_k(n), \quad (22)$$

with $\mathbf{Z}(n)$ satisfying (H1) and (H2) as before.

By definition, $\mathbf{Y}_k(n)$ and $\mathbf{Q}_k(n)$ are updated at the $(n+1)$ -th update period if and only if $k \in \mathcal{K}_n$, so every user only needs to keep track of his individual update timer. In this way, we obtain the following decentralized variant of Algorithm 1 (shown here for a single, focal transmitter and with step sizes of the form $\gamma_n = \gamma/n$ for simplicity):

Algorithm 2 Asynchronous exponential learning (MXL-a).

Parameter: $\gamma > 0$.

Initialize: $n \leftarrow 0$; $\mathbf{Y} \leftarrow \mathbf{0}$; $\mathbf{Q} \leftarrow \frac{P}{M} \cdot \mathbf{I}$

Repeat

```

foreach UpdateEvent do
   $n \leftarrow n + 1$ ;
  receive estimate  $\hat{\mathbf{V}}$  of  $\mathbf{V}$ ;
  update score matrix:  $\mathbf{Y} \leftarrow \mathbf{Y} + \gamma/n \cdot \hat{\mathbf{V}}$ ;
  set covariance matrix:  $\mathbf{Q} \leftarrow P \exp(\mathbf{Y}) / \text{tr}[\exp(\mathbf{Y})]$ ;
until termination criterion is reached.

```

Remarkably, in this asynchronous context (with delayed, imperfect measurements), we still get:

Theorem 2. *Assume that the users' delay processes $d_k(n)$ are bounded (a.s.) and that the set of users \mathcal{K}_n that update at step n is a homogeneous recurrent Markov chain – i.e. every user updates at a positive rate. Then, the iterates of Algorithm 2 converge almost surely to $\arg \max_{\mathbf{Q}} R(\mathbf{Q})$.*

Proof: See Appendix C. ■

Obviously, Algorithm 2 enjoys the same implementation properties as Algorithm 1, and, in addition:

(P5) *Asynchronicity*: there is no need for a global update timer to synchronize the network’s wireless users.

In particular, the criteria that trigger an UpdateEvent could be completely arbitrary, so (MXL-a) is more suitable for scenarios where there can be no coordination between the transmitters’ update periods. Otherwise, if an UpdateEvent is triggered simultaneously (e.g. if it is triggered by the receiver’s broadcasts), Algorithm 2 reduces to synchronous MXL (Alg. 1): in this case, the algorithm’s convergence can be greatly sped up because more users update per period.

D. Eigenvalues, eigenvectors and learning

We close this section by describing the evolution of the users’ transmit eigenvectors and eigenvalues under (MXL) and using this description to propose an alternative implementation of Algorithm 1. The key ingredient of our analysis is the following proposition:

Proposition 1. *Let $\{q_{k\alpha}, \mathbf{u}_{k\alpha}\}_{\alpha=1}^{M_k}$ be a smooth eigen-system for \mathbf{Q}_k and let $V_{\alpha\beta}^k \equiv \mathbf{u}_{k\alpha}^\dagger \mathbf{V}_k \mathbf{u}_{k\beta}$. Then, the iterates of Algorithm 1 track the mean dynamics:*

$$\dot{q}_{k\alpha} = q_{k\alpha} \left(V_{\alpha\alpha}^k - P_k^{-1} \sum_{\beta=1}^{M_k} q_{k\beta} V_{\beta\beta}^k \right), \quad (23a)$$

$$\dot{\mathbf{u}}_{k\alpha} = \sum_{\beta \neq \alpha} V_{\beta\alpha}^k \left(\log q_{k\alpha} - \log q_{k\beta} \right)^{-1} \mathbf{u}_{k\beta}. \quad (23b)$$

Proof: See Appendix C. ■

The precise sense in which $\mathbf{Q}(n)$ “tracks” the mean dynamics (23) is explained in Appendix A; for our purposes, the most important consequence of Proposition 1 is that (23) leads to the following variant of Algorithm 1:

Algorithm 3 Eigen-based exponential learning (MXL-eig).

Parameter: decreasing step-size sequence γ_n

Initialize: $n \leftarrow 0$; $q_{k\alpha}$; $\mathbf{u}_{k\alpha}$

Repeat

$n \leftarrow n + 1$;

foreach user $k \in \mathcal{K}$ do

measure \mathbf{V}_k ;

update eigenvalues: $q_{k\alpha} \leftarrow q_{k\alpha} + \gamma_n q_{k\alpha} \left(V_{\alpha\alpha}^k - P_k^{-1} \sum_{\beta=1}^{M_k} q_{k\beta} V_{\beta\beta}^k \right)$;

update eigenvectors: $\mathbf{u}_{k\alpha} \leftarrow \mathbf{u}_{k\alpha} + \gamma_n \sum_{\beta \neq \alpha} V_{\beta\alpha}^k \left(\log q_{k\alpha} - \log q_{k\beta} \right)^{-1} \mathbf{u}_{k\beta}$;

correct roundoff errors: $\mathbf{u} \leftarrow \text{Orthonormal}(\mathbf{u})$;

set covariance matrix $\mathbf{Q}_k \leftarrow \sum_{\alpha=1}^{M_k} q_{k\alpha} \mathbf{u}_{k\alpha} \mathbf{u}_{k\alpha}^\dagger$;

until termination criterion is reached.

As in the case of the original MXL algorithm, we then obtain:

Theorem 3. Assume that Algorithm 3 is run with sufficiently small, nonincreasing step-sizes γ_n such that $\sum_n \gamma_n^2 < \infty$ and $\sum_n \gamma_n = \infty$. Then, $\mathbf{Q}(n)$ converges almost surely to $\arg \max_{\mathbf{Q}} R(\mathbf{Q})$.

We close this section with a few remarks on Algorithm 3:

a) *The orthonormalization step:* Even though the eigenvector dynamics (23b) preserve orthonormality, Algorithm 3 introduces an $O(\gamma_n^2)$ round-off error to orthogonality due to discretization. The call to `Orthonormal` performs a basis orthonormalization and it is intended to correct that error in order to yield a covariance matrix \mathbf{Q}_k that satisfies the feasibility constraints (7) of (RM): like matrix exponentiation, orthonormalization has the same complexity as matrix multiplication (fast Coppersmith–Winograd methods [25] provide an $O(M_k^{2.373})$ bound), so this does not increase the algorithm’s (polynomial) complexity.

b) *Noisy measurements:* Theorem 3 has been stated for simplicity for noiseless measurements. In the case of noisy measurements, the step-size of the algorithm must be tuned adaptively so that $q_{k\alpha} \geq 0$; it is not hard to do so by using the random step-size techniques of [14], but we chose to focus on the noiseless case for presentational clarity.

IV. THE CASE OF FAST-FADING CHANNELS

In the presence of fading, the users’ channel matrices \mathbf{H}_k evolve stochastically over time at a rate which is much faster than the characteristic length of each transmission block; as a result, the static sum rate function R of (8) is no longer relevant. In this case, the users’ achievable sum rate for fixed \mathbf{Q} under fast fading is given by the ergodic average [2, 28]:

$$R_{\text{erg}}(\mathbf{Q}) = \mathbb{E}_{\mathbf{H}} \left[\log \det \left(\mathbf{I} + \sum_k \mathbf{H}_k \mathbf{Q}_k \mathbf{H}_k^\dagger \right) \right], \quad (24)$$

where the expectation is now taken with respect to the law of \mathbf{H} (assumed here to follow a stationary, ergodic process). Accordingly, we obtain the ergodic rate maximization problem for fast-fading channels:

$$\begin{aligned} & \text{maximize} && R_{\text{erg}}(\mathbf{Q}), \\ & \text{subject to} && \mathbf{Q}_k \in \mathcal{X}_k, \quad k = 1, \dots, K, \end{aligned} \quad (\text{ERM})$$

where the users’ feasible sets \mathcal{X}_k are defined as in (7): $\mathcal{X}_k = \{\mathbf{Q}_k \succeq 0 : \text{tr}(\mathbf{Q}_k) = P_k\}$.⁹

Since expectation preserves convexity, the ergodic rate maximization problem (ERM) remains concave – in fact, it is straightforward to show that (ERM) is *strictly* concave [29]. However, given that the integration over the law of \mathbf{H} is typically impossible to carry out, calculating the ergodic gradient $\mathbf{V}_{\text{erg}} = \nabla R_{\text{erg}}$ of R_{erg} is a likewise impractical task. Thus, instead of relying on intricate analytic calculations (that require substantial computation capabilities and a good deal of knowledge regarding the channels’ statistics), we will consider the same sequence of events as in the case of static channels:

1) At every update period $n = 1, 2, \dots$, each user $k \in \mathcal{K}$ gets an estimate $\hat{\mathbf{V}}_k(n)$ of the matrix

$$\mathbf{V}_k(n) = \mathbf{H}_k^\dagger(n) \left[\mathbf{I} + \sum_{\ell} \mathbf{H}_\ell(n) \mathbf{Q}_\ell(n) \mathbf{H}_\ell^\dagger(n) \right]^{-1} \mathbf{H}_k(n), \quad (25)$$

⁹Perhaps more appropriately for the case of interest, the above expression also holds over the long term for block-fading channels, in which case the channel is essentially fixed over each transmission length during which the instantaneous rate is used.

where $\mathbf{H}_k(n)$ denotes the instantaneous realization of the channel matrix of user k at period n .

- 2) Users update their signal covariance matrices according to the recursion (MXL) and the process repeats until a termination criterion is reached.

Formally, writing $\mathbf{Z}_k(n) = \hat{\mathbf{V}}_k(n) - \mathbb{E}[\mathbf{V}_k(n)]$ for the difference between the users' observed estimate $\hat{\mathbf{V}}_k(n)$ and the expected value of (25), we will make the same statistical hypotheses for \mathbf{Z} as in the static regime – though we should note here that fluctuations are now due to *both measurement errors and the channels' inherent variability*. Quite remarkably, despite the change of objective function, we obtain the following convergence result for fast-fading channels:

Theorem 4. *Assume that Algorithm 1 is run with nonincreasing step-sizes γ_n such that $\sum_n \gamma_n^2 < \sum_n \gamma_n = \infty$ and noisy measurements $\hat{\mathbf{V}}(n)$ satisfying hypotheses (H1) and (H2) with respect to (25). Then, $\mathbf{Q}(n)$ converges almost surely to the solution of the ergodic rate maximization problem (ERM); moreover, the conclusions of Theorem 1 for an arbitrary nonincreasing step-size sequence γ_n also hold with the static sum rate R replaced by the ergodic sum rate R_{erg} .*

Proof: See Appendix D. ■

In view of Theorem 4, we see that Algorithm 2 enjoys the additional property:

(P6) *Flexibility:* the MXL algorithm can be applied “as-is” in both static and fast-fading channels.

In particular, the same convergence rate and large deviation estimates that were derived for static channels in the previous section (cf. the remarks following Theorem 1) also carry over to the fast-fading regime – as does the analysis of Secs. III-B, III-C and III-D for the users' measurement process and for the asynchronous and eigen-based variants of MXL respectively. The only difference here is that the variance σ that appears e.g. in (14) and (16) is not only due to imperfections in the estimation process of \mathbf{V} , but also stems from the inherent variability of the system's channels due to fast-fading. We will explore this issue in the following section.

V. NUMERICAL SIMULATIONS

To validate the theoretical analysis of the previous sections and to assess the performance of the MXL algorithm (Alg. 1) in practical scenarios, we conducted extensive numerical simulations from which we illustrate here a selection of the most representative cases.

First, in Figure 1, we investigate the convergence speed of MXL as a function of the number of wireless transmitters, using existing water-filling (WF) methods as a benchmark. To that end, we simulated a multi-user uplink MIMO system consisting of a single receiver with $N = 24$ antennas and different numbers of wireless transmitters, each with a random number of transmit antennas, chosen randomly between 2 and 8 (due to space limitations, we only present here the case of $K = 20$ and $K = 50$ users). The users' channel matrices \mathbf{H}_k were then drawn from a complex Gaussian distribution at the outset of the process and were kept fixed throughout the transmission horizon.¹⁰

¹⁰For simplicity, we neglect effects of path-loss in this simulation. This treatment is reasonable if we assume that users “invert” their pathloss function by appropriately compensating their total transmission power level P_k [30].

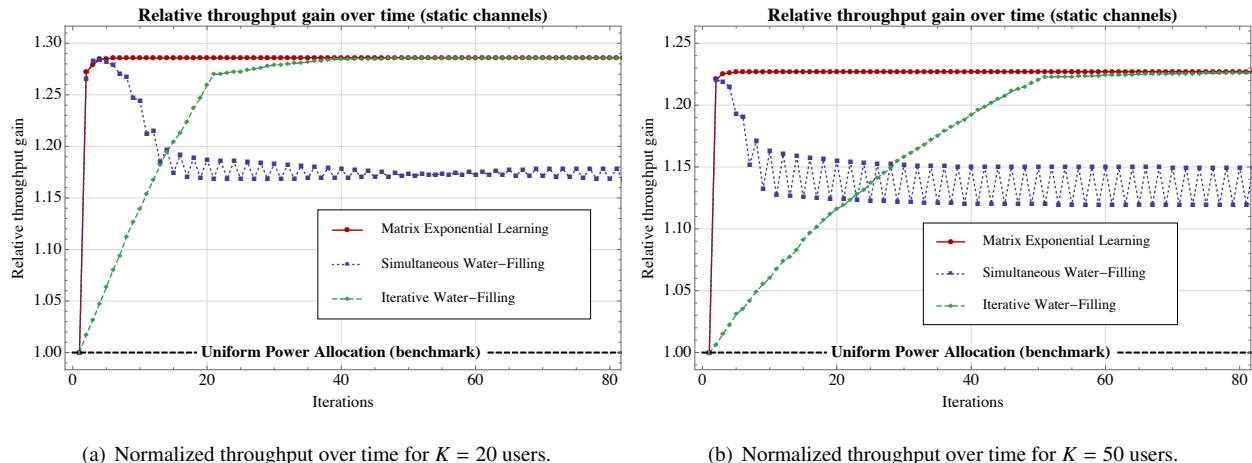


Fig. 1. Comparison of matrix exponential learning (MXL) to water-filling (WF) methods. The classical IWF algorithm converges relatively slowly (roughly within $O(K)$ iterations) because only one user updates per cycle; the SWF variant is much faster (because all users updates simultaneously), but it may fail to converge due to the appearance of best-response cycles in the update process. By contrast, we see that the MXL algorithm converges within a few iterations, even for large numbers of users.

For comparison purposes, we ran Algorithm 1 with constant step size alongside the classical iterative water-filling algorithm proposed in [8] and the simultaneous variant of [23], initializing all methods with a uniform power allocation profile that assigns the same power to all transmit antennas (the benchmark case). The algorithms' performance over time was then assessed by plotting the normalized throughput gain

$$r_n = R_n/R_0, \quad (26)$$

where R_n denotes the system's sum rate at the n -th iteration of the algorithm, and the benchmark rate R_0 denotes the system's sum rate when all users employ a uniform beamforming policy.

As can be seen in Fig. 1, the MXL algorithm attains the system's sum capacity within a few iterations (effectively, within a *single* iteration for $K = 50$ users).¹¹ This convergence behavior represents a marked improvement over traditional WF methods, even in moderately-sized systems with $K = 20$ users: on the one hand, IWF is significantly slower than MXL (it requires $O(K)$ iterations to achieve the same performance level as the first iteration of MXL), whereas SWF may fail to converge altogether due to “ping-pong” effects where users overcommit to a given spatial direction by diverting too much power to it all at once (thus “congesting” it) and then switch transmit directions in an effort to exploit the ensuing spatial gap (thus relinquishing the benefits from employing it in the first place).¹²

In Figure 2, we investigate the robustness of MXL under imperfect signal and channel measurements, and we compare it to iterative and simultaneous WF methods under similar conditions. Specifically, in Fig. 2, we simulated a multi-user uplink MIMO system consisting of a single receiver with $N = 24$ antennas and $K = 20$ wireless transmitters with antenna and channel characteristics as in Fig. 1. To simulate noisy measurements, we used the estimation scheme

¹¹Alternatively, in the game-theoretic context of (NE), this implies that the system's users reach a unilaterally stable Nash equilibrium.

¹²For a detailed account of best-response cycles of this kind, see e.g. [31].

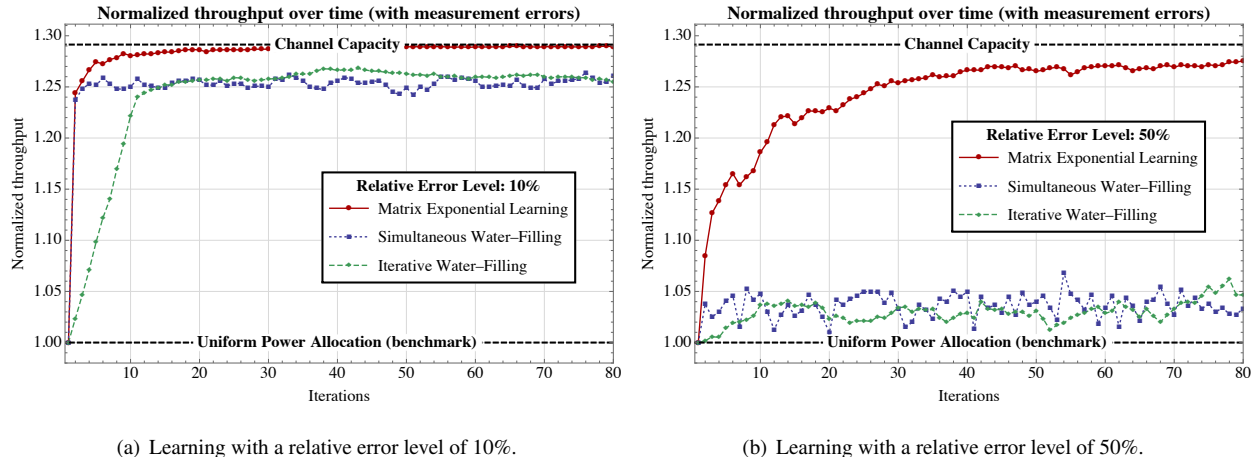


Fig. 2. Performance of matrix exponential learning and water-filling (WF) methods under imperfect CSI. In contrast to WF methods, the MXL algorithm attains the channel’s sum capacity, even in the presence of very high measurement errors.

of Section III-B where the received signal precision matrix $\mathbf{P} = \mathbb{E}[\mathbf{y}\mathbf{y}^\dagger]^{-1}$ of Eq. (18) is estimated by sampling the aggregate signal \mathbf{y} at the receiver and then feeding the unbiased sample mean (19) to the transmitters. The measurement noise was controlled by the relative error level of the estimator (deviation/mean), so a relative error level of η means that, on average, the estimated matrix lies within $\eta\%$ of its true value (in terms of the Frobenius matrix norm). We then plotted the efficiency of MXL over time for average error levels of $\eta = 10\%$ and $\eta = 50\%$, and we ran the iterative and simultaneous WF algorithms with the same sample realizations for comparison.

As can be seen in Figure 2, the performance of water-filling methods remains acceptable at low error levels, allowing users to attain between 90% and 95% of the channel’s sum capacity. However, when the measurement error level gets higher, water-filling (either iterative or simultaneous) offers no perceptible advantage over the users’ initial signal covariance matrices (the benchmark case of uniform power allocation across antennas). By contrast, as predicted by Theorem 1, the MXL algorithm retains its convergence properties and converges to the system’s sum capacity, even under very noisy measurements – though, of course, the algorithm’s convergence speed is negatively impacted when the measurement noise grows too high.

Finally, to account for time-varying channel conditions, we also plotted the performance of the proposed MXL algorithm in non-static channels, following the well-known Jakes model for Rayleigh fading [32]. Specifically, in Figure 3, we consider a MIMO uplink system consisting of a receiver with $N = 8$ antennas and $K = 10$ mobile users with 2 transmit antennas, each transmitting at a central frequency of $f = 2$ GHz. For the users’ mobility model, we used the extended pedestrian A (EPA) and extended vehicular A (EVA) models [33] with average user velocities $v = 5$ m/s (pedestrian movement) and $v = 15$ m/s (vehicular movement in traffic-heavy urban environments). We then ran the MXL algorithm with an update period of $\delta = 5$ ms (one update per frame), and we plotted the algorithm’s achieved sum rate R_n at the n -th iteration of the algorithm versus *a*) the system’s sum capacity R_n^{\max} given the current realization of the channel matrices $\mathbf{H}_k(t)$ at time $t = n\delta$; and *b*) the users’ sum rate under uniform power allocation over

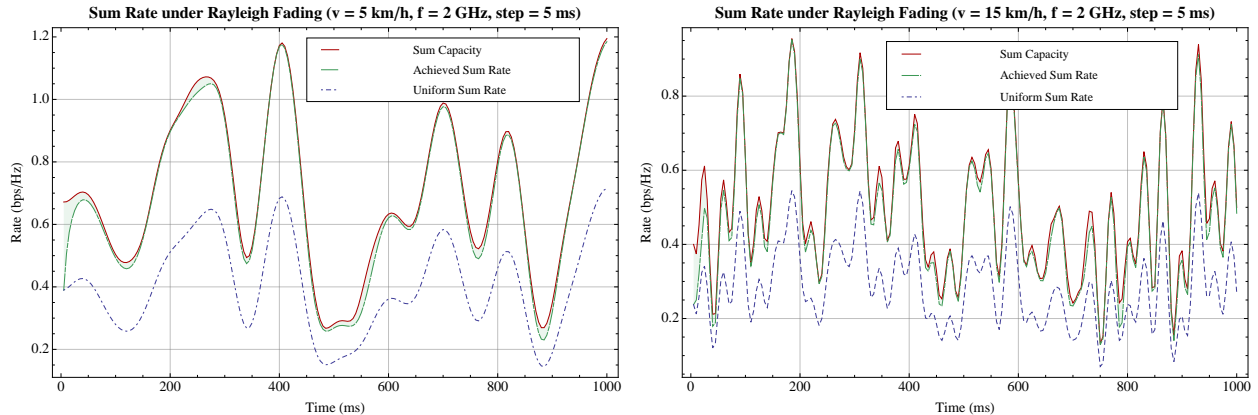
(a) Performance of MXL with average user velocity $v = 5$ m/s.(b) Performance of MXL with average user velocity $v = 15$ m/s.

Fig. 3. Data rates achieved by MXL in a dynamic environment with time-varying channels following the Jakes model for Rayleigh fading (model parameters indicated in the figure caption). The dynamic transmit policy induced by the MXL algorithm allows users to track the system's sum capacity remarkably well, even under rapidly changing channel conditions.

their antennas. Thanks to its high convergence speed and its robustness, the MXL algorithm tracks the system's sum capacity remarkably well, despite the channels' variability. Moreover, the throughput difference between the learned transmit covariance profile and the uniform one shows that this tracking is not an artifact of the system's sum capacity falling within a narrow band of what could be attained by spreading power uniformly over antennas: users actively track the system's optimum transmit profile as it evolves over time, even under rapidly varying channel conditions.

VI. CONCLUSIONS AND PERSPECTIVES

In this paper, we introduced a distributed signal covariance optimization algorithm to maximize the uplink sum capacity of multi-antenna users that transmit to a common multi-antenna receiver with only imperfect, possibly delayed and asynchronously updated channel state information at the users' disposal. Under fairly mild hypotheses for the moments of the statistics of the estimation imperfections, we showed that the proposed matrix exponential learning (MXL) algorithm converges rapidly, even for large numbers of users and/or antennas per user; moreover, the probability that the algorithm deviates beyond a small error from the optimum after a fixed number of iterations is very small (and decays exponentially if the moments of the error process do not grow too fast). In our view, these robustness properties of MXL make it an attractive alternative to water-filling methods that may fail to converge altogether in the presence of measurement noise. This is confirmed by extensive numerical simulations which exhibit the fast convergence and robustness properties of MXL in realistic channel conditions.

We focused on the MIMO multiple access channel only for simplicity. The proposed algorithm can be readily extended to a MIMO-OFDM framework, different precoding schemes (such as MMSE or ZF-type precoders) or to account for other transmission features such as spectral mask constraints, pricing, etc. The method can also be adapted to wide range channel models (such as the interference channel), where a game-theoretic approach as in [9, 22] is more

appropriate: in this context, a natural question that arises is whether the algorithm converges to a Nash equilibrium, and whether this convergence is retained in the presence of noise. In fact, thanks to the exponentiation step, our method can be adapted to even more general constrained matrix optimization problems as in [34, 35]; we intend to explore these directions in future work.

APPENDIX
TECHNICAL PROOFS

Our goal in this appendix will be to prove the convergence results presented in the rest of our paper. To that end, we will first establish the convergence of a deterministic, “mean-field” dynamical system associated to the MXL algorithm, and we will then show that the iterates of MXL and its variants comprise a stochastic approximation thereof [14]. Our robustness results will then follow by exploiting the powerful martingale concentration inequalities of [19].

For notational clarity, in the rest of this appendix (and unless explicitly stated otherwise), we will treat the case of a single user with maximum transmit power $P = 1$; the general case is simply a matter of taking a direct sum over $k \in \mathcal{K}$ and rescaling by the corresponding maximum power P_k .

A. The mean dynamics of exponential learning

We begin by considering the following continuous-time version of the basic recursion (MXL):

$$\begin{aligned} \dot{\mathbf{Y}} &= \mathbf{V}, \\ \mathbf{Q} &= \frac{\exp(\mathbf{Y})}{\text{tr}[\exp(\mathbf{Y})]}, \end{aligned} \tag{MXL-c}$$

The following proposition shows that (MXL-c) converges to the solution set of the rate maximization problem (RM):

Theorem 5. *Let $\mathbf{Q}(t)$ be a solution orbit of (MXL-c). Then, $\mathbf{Q}(t)$ converges to a minimizer of (RM).*

A key ingredient in our proof will be the (negative) von Neumann quantum entropy:

$$h(\mathbf{Q}) = \text{tr}[\mathbf{Q} \log \mathbf{Q}], \quad \mathbf{Q} \in \mathcal{Q}, \tag{27}$$

and its convex conjugate (Legendre transform):¹³

$$h^*(\mathbf{Y}) \equiv \max_{\mathbf{Q} \in \mathcal{Q}} \{\text{tr}[\mathbf{Y}\mathbf{Q}] - h(\mathbf{Q})\} = \log \text{tr}[\exp(\mathbf{Y})], \tag{28}$$

where \mathcal{Q} denotes the (compact) spectrahedron:

$$\mathcal{Q} = \{\mathbf{Q} \succeq 0 : \text{tr}(\mathbf{Q}) = 1\}. \tag{29}$$

It will also be convenient to introduce the following “primal-dual” coupling between \mathbf{Q} and \mathbf{Y} :

$$F(\mathbf{Q}, \mathbf{Y}) = h(\mathbf{Q}) + h^*(\mathbf{Y}) - \text{tr}[\mathbf{Q}\mathbf{Y}]. \tag{30}$$

¹³The convexity of $h(\mathbf{Q})$ is well known [36]. To derive the expression (28) for its conjugate, simply note that $h(\mathbf{Q}) = \sum_j q_j \log q_j$ where q_j are the eigenvalues of \mathbf{Q} ; Eq. (28) then follows from the expression $h^*(y) = \log \sum_j \exp(y_j)$ for the Legendre transform of the (negative) Gibbs entropy.

Eq. (30) gathers all the terms of Fenchel's inequality [37], so, following [38], we will refer to it as the *Fenchel coupling* between \mathbf{Q} and \mathbf{Y} . Below, we present some key properties of F :

Lemma 1. *With notation as above, we have $F(\mathbf{Q}, \mathbf{Y}) \geq 0$ with equality iff $\mathbf{Q} = \exp(\mathbf{Y}) / \text{tr}[\exp(\mathbf{Y})]$. Moreover:*

$$\nabla_{\mathbf{Y}} h^*(\mathbf{Y}) = \frac{\exp(\mathbf{Y})}{\text{tr}[\exp(\mathbf{Y})]}, \quad (31)$$

and

$$\nabla_{\mathbf{Y}} F(\mathbf{Q}, \mathbf{Y}) = \frac{\exp(\mathbf{Y})}{\text{tr}[\exp(\mathbf{Y})]} - \mathbf{Q}. \quad (32)$$

Proof: By standard matrix analysis results [39], we have:

$$\nabla_{\mathbf{Y}} h^*(\mathbf{Y}) = \frac{1}{\text{tr}[\exp(\mathbf{Y})]} \nabla_{\mathbf{Y}} \text{tr}[\exp(\mathbf{Y})] = \frac{\exp(\mathbf{Y})}{\text{tr}[\exp(\mathbf{Y})]}, \quad (33)$$

and (32) follows trivially. The first part of our claim is then a consequence of the general theory of convex conjugation – see e.g. [37, Chap. 26]. ■

Proof of Theorem 5: Our proof relies on the fact that the Fenchel coupling $H(t) = F(\mathbf{Q}^*, Y(t))$ is a Lyapunov function for (MXL-c) for every maximizer \mathbf{Q}^* of (RM). Indeed, the definition of the Fenchel coupling and Lemma 1 yield

$$\dot{H} = \text{tr}[\nabla_{\mathbf{Y}} h^*(\mathbf{Y}) \cdot \dot{\mathbf{Y}}] - \text{tr}[\mathbf{Q}^* \dot{\mathbf{Y}}] = \text{tr}[(\mathbf{Q} - \mathbf{Q}^*) \cdot \nabla_{\mathbf{Q}} R] \leq 0, \quad (34)$$

where the inequality in the last step follows from the concavity of R and the fact that \mathbf{Q}^* is a maximizer of R . Moreover, equality in (34) holds if and only if \mathbf{Q} is also a maximizer of R , so H is a Lyapunov function for (MXL-c) with respect to $\arg \max R$.

The above reasoning shows that (MXL-c) converges to $\arg \max R$, but since R is not necessarily strictly concave, this does not imply that every trajectory of (MXL-c) converges to a specific point in $\arg \max R$. To show that this is indeed the case, let $\mathbf{Q}(t)$ be an orbit of (MXL-c) and let \mathbf{Q}^* be an ω -limit of $\mathbf{Q}(t)$, i.e. $\mathbf{Q}(t_n) \rightarrow \mathbf{Q}^*$ for some increasing sequence $t_n \rightarrow \infty$. By Lemma 1, this implies that $F(\mathbf{Q}^*, \mathbf{Y}(t_n)) \rightarrow 0$, so, since $F(\mathbf{Q}^*, \mathbf{Y}(t))$ is nonincreasing, we also get $\lim_{t \rightarrow \infty} F(\mathbf{Q}^*, \mathbf{Y}(t)) = 0$. We conclude that $\mathbf{Q}(t) \rightarrow \mathbf{Q}^*$ (again by Lemma 1) and our proof is complete. ■

B. Stochastic approximation and convergence

We now proceed to show that the iterates of the MXL are asymptotically close to solution segments of (MXL-c) of arbitrary length – more precisely, that they comprise an asymptotic pseudotrajectory (APT) of (MXL-c) in the sense of [14].

Proposition 2. *Assume that (MXL) is run with a nonincreasing step-size sequence γ_n such that $\sum_n \gamma_n^2 < \sum_n \gamma_n = +\infty$ and noisy measurements $\hat{\mathbf{V}}_k$ satisfying (H1) and (H2). Then, the iterates $\mathbf{Q}(n)$ of (MXL) form an asymptotic pseudotrajectory of (MXL-c).*

Proof: Simply note that the recursion (MXL) can be written in the form:

$$\mathbf{Y}(n+1) = \mathbf{Y}(n) + \gamma_n [\mathbf{V}(\mathbf{Q}(n)) + \mathbf{Z}(n)]. \quad (35)$$

Since the map $\mathbf{Y} \mapsto \mathbf{Q}$ is Lipschitz¹⁴ and the rate function $R(\mathbf{Q})$ is smooth over the compact spectrahedron \mathcal{Q} , it follows that the map $\mathbf{Y} \mapsto \mathbf{V}(\mathbf{Q}(\mathbf{Y}))$ is Lipschitz and bounded. Our claim then follows from Propositions 4.2 and 4.1 in [14]. \blacksquare

With all this said and done, we are finally in a position to prove Theorem 1:

Proof of Theorem 1: Let $\mathcal{Q}^* = \arg \max_{\mathbf{Q} \in \mathcal{Q}} R(\mathbf{Q})$ denote the solution set of (RM) and assume ad absurdum that $\mathbf{Q}(n)$ remains a bounded distance away from \mathcal{Q}^* . Furthermore, fix some $\mathbf{Q}^* \in \mathcal{Q}^*$ and let $D_n = F(\mathbf{Q}, \mathbf{Y}(n))$; a Taylor expansion of F then yields:

$$\begin{aligned} D_{n+1} &= F(\mathbf{Q}^*, \mathbf{Y}(n+1)) = F(\mathbf{Q}^*, \mathbf{Y}(n) + \gamma_n \hat{\mathbf{V}}(n)) \\ &\leq D_n + \gamma_n \operatorname{tr}[(\mathbf{Q}(n) - \mathbf{Q}^*) \cdot \mathbf{V}(\mathbf{Q}(n))] + \gamma_n \xi_n + \frac{1}{2} \gamma_n^2 \|\hat{\mathbf{V}}(n)\|^2, \end{aligned} \quad (36)$$

where $\xi_n = \operatorname{tr}[\mathbf{Z}(n) \cdot (\mathbf{Q}^* - \mathbf{Q}(n))]$ and we have used the fact that the convex conjugate h^* of the von Neumann entropy is 1-strongly smooth [17].

Our original assumption that $\mathbf{Q}(n)$ remains a bounded distance away from \mathcal{Q}^* means that D_n is bounded away from zero; moreover, with R concave and smooth, we will also have $\operatorname{tr}[\mathbf{V}(n) \cdot (\mathbf{Q}(n) - \mathbf{Q}^*)] \leq -m$ for some $m > 0$. Thus, telescoping (36) yields:

$$D_{n+1} \leq D_0 - t_n \left(m - \sum_{j=1}^n w_{j,n} \xi_j \right) + \frac{1}{2} \sum_{j=1}^n \gamma_j^2 \|\hat{\mathbf{V}}(j)\|^2, \quad (37)$$

where $t_n = \sum_{j=1}^n \gamma_j$ and $w_{j,n} = \gamma_j / t_n$. By the strong law of large numbers for martingale differences [18, Theorem 2.18], we have $n^{-1} \sum_{j=1}^n \xi_j \rightarrow 0$ (a.s.); hence, with $\gamma_{n+1}/\gamma_n \leq 1$, Hardy's Tauberian summability criterion [40, p. 58] applied to the weight sequence $w_{j,n} = \gamma_j / t_n$ yields $\sum_{j=1}^n w_{j,n} \xi_j \rightarrow 0$ (a.s.). Finally, since γ_n is square-summable and $\gamma_n \mathbf{Z}(n)$ is a martingale difference with finite variance, it follows that $\sum_{n=1}^{\infty} \gamma_n^2 \|\hat{\mathbf{V}}(n)\|^2 < \infty$ (a.s.) by Theorem 6 in [41].

Combining all of the above, we see that the RHS of (37) tends to $-\infty$ (a.s.); this contradicts the fact that $D_n \leq 0$, so we conclude that $\mathbf{Q}(n)$ visits a compact neighborhood of \mathcal{Q}^* infinitely often. Since \mathcal{Q}^* attracts any initial condition $\mathbf{Y}(0)$ under the continuous-time dynamics (MXL), Theorem 6.10 in [14] shows that $\mathbf{Q}(n)$ converges to \mathcal{Q}^* , as claimed.

For the bound (13), note that (36) can be rewritten as

$$\gamma_n \operatorname{tr}[(\mathbf{Q}^* - \mathbf{Q}(n)) \cdot \mathbf{V}(\mathbf{Q}(n))] \leq D_n - D_{n+1} + \gamma_n \xi_n + \frac{1}{2} \gamma_n^2 \|\hat{\mathbf{V}}(n)\|^2, \quad (38)$$

so, recalling that R is concave and $\mathbf{V} = \nabla_{\mathbf{Q}} R$, we get:

$$\begin{aligned} \gamma_n [R_{\max} - R_n] &\leq \gamma_n \operatorname{tr}[(\mathbf{Q}^* - \mathbf{Q}(n)) \cdot \mathbf{V}(\mathbf{Q}(n))] \\ &\leq D_n - D_{n+1} + \gamma_n \xi_n + \frac{1}{2} \gamma_n^2 \|\hat{\mathbf{V}}(n)\|^2. \end{aligned} \quad (39)$$

Thus, taking expectations on both sides and telescoping, we obtain:

$$\sum_{j=1}^n \gamma_j [R_{\max} - \mathbb{E}[R_j]] \leq D_0 + \frac{1}{2} V^2 \sum_{j=1}^n \gamma_j^2, \quad (40)$$

¹⁴This follows from the fact that the von Neumann entropy (27) is strongly convex with respect to the nuclear norm [17, 24].

where we have used the fact that $\mathbb{E}[\xi_n] = 0$ and the finite mean square hypothesis $\mathbb{E}[\|\hat{\mathbf{V}}(n)\|^2] \leq V^2$. From (30), we have $D_0 = F(\mathbf{Q}^*, 0) \leq \max_{\mathbf{Q}, \mathbf{Q}'} \{h(\mathbf{Q}) - h(\mathbf{Q}')\} = \log M$, so (13) follows by rearranging (40) and solving for $\mathbb{E}[\bar{R}_n] = t_n^{-1} \sum_{j=1}^n \gamma_j \mathbb{E}[R_j]$.

Moreover, for the large deviations bound (14), Eq. (39) yields $R_{\max} - \bar{R}_n \leq \varepsilon_n + t_n^{-1} \sum_{j=1}^n \gamma_j \xi_j$, so

$$\mathbb{P}(R_{\max} - \bar{R}_n \geq \varepsilon_n + z) \leq \mathbb{P}\left(\sum_{j=1}^n |\gamma_j \xi_j| \geq t_n z\right), \quad (41)$$

with $\varepsilon_n = t_n^{-1} \left(\log M + \frac{1}{2} V^2 \sum_{j=1}^n \gamma_j^2\right)$ defined as in (15). Since $\gamma_j \xi_j$ is a martingale difference with finite conditional variance $\text{Var}(\gamma_j \xi_j) \leq A \gamma_j^2 \sigma^2$ for some $A > 0$, Chebyshev's inequality yields:

$$\mathbb{P}\left(\sum_{j=1}^n |\gamma_j \xi_j| \geq t_n z\right) \leq \frac{1}{t_n^2 z^2} \sum_{j=1}^n \text{Var}(\gamma_j \xi_j) \leq \frac{A \sigma^2}{t_n^2 z^2} \sum_{j=1}^n \gamma_j^2 = \mathcal{O}\left(\sigma^2 z^{-2} t_n^{-2} \sum_{j=1}^n \gamma_j^2\right). \quad (42)$$

Finally, if the conditional distribution of $\hat{\mathbf{V}}(n)$ given $\mathbf{Q}(n-1)$ is symmetric around $\mathbf{V}(\mathbf{Q}(n-1))$, the conditional distribution of ξ_n will be symmetric around 0, so the bound (16) follows from the exponential concentration inequality (6.1) of [19]. Otherwise, under the modified hypothesis (H2'), the exponential bound (16) follows from Theorem 1.2A in [19]. ■

C. Variants of MXL

In this section, we prove the convergence of the variant exponential learning schemes MXL-a and MXL-eig (Algorithms 2 and 3 respectively).

Proof of Theorem 2: We will show that the recursion (MXL-a) is an asynchronous stochastic approximation of (MXL-c) in the sense of [15, Chap. 7]. Indeed, by Theorems 2 and 3 in [15], the recursion (MXL-a) may be viewed as a stochastic approximation of the rate-adjusted dynamics

$$\begin{aligned} \dot{\mathbf{Y}}_k &= \eta_k \mathbf{V}_k \\ \mathbf{Q}_k &= \frac{\exp(\mathbf{Y}_k)}{\text{tr}[\exp(\mathbf{Y}_k)]} \end{aligned} \quad (43)$$

where we have momentarily reinstated the user index k and $\eta_k = \lim_{n \rightarrow \infty} n_k/n > 0$ denotes the update rate of user k (the existence and positivity of this limit follows from the ergodicity of the update process \mathcal{K}_n). This multiplicative factor does not alter the rest points and internally chain transitive (ICT) sets [14] of the dynamics (MXL-c), so (43) converges to $\arg \max R$ from any initial condition and the proof of Theorem 1 carries through essentially verbatim. ■

To prove Theorem 3, we first need to derive the eigen-dynamics (23) induced by (MXL-c):

Proposition 3. *Let $\mathbf{Q}(t)$ be a solution orbit of (MXL-c) and let $\{q_\alpha(t), \mathbf{u}_\alpha(t)\}$ be a smooth eigen-decomposition of $\mathbf{Q}(t)$. Then, $\{q_\alpha(t), \mathbf{u}_\alpha(t)\}$ is a solution of the eigen-dynamics (23).*

Proof: By differentiating the identity $q_\alpha \delta_{\alpha\beta} = \mathbf{u}_\alpha^\dagger \mathbf{Q} \mathbf{u}_\beta$, we readily obtain:

$$\begin{aligned} \dot{q}_\alpha \delta_{\alpha\beta} &= \dot{\mathbf{u}}_\alpha^\dagger \mathbf{Q} \mathbf{u}_\beta + \mathbf{u}_\alpha^\dagger \dot{\mathbf{Q}} \mathbf{u}_\beta + \mathbf{u}_\alpha^\dagger \mathbf{Q} \dot{\mathbf{u}}_\beta \\ &= \mathbf{u}_\alpha^\dagger \dot{\mathbf{Q}} \mathbf{u}_\beta + (q_\alpha - q_\beta) \mathbf{u}_\alpha^\dagger \dot{\mathbf{u}}_\beta, \end{aligned} \quad (44)$$

where the last equality follows by differentiating the orthogonality condition $\mathbf{u}_\alpha^\dagger \mathbf{u}_\beta = \delta_{\alpha\beta}$. Thus, by a) taking $\alpha = \beta$ and b) solving for $\dot{\mathbf{u}}_\alpha^\dagger$ in (44), we respectively obtain:

$$\dot{q}_\alpha = \mathbf{u}_\alpha^\dagger \dot{\mathbf{Q}} \mathbf{u}_\alpha \quad (45a)$$

$$\dot{\mathbf{u}}_\alpha^\dagger = \sum_{\beta \neq \alpha} \frac{\mathbf{u}_\alpha^\dagger \dot{\mathbf{Q}} \mathbf{u}_\beta}{q_\alpha - q_\beta} \mathbf{u}_\beta^\dagger \quad (45b)$$

However, by using the Fréchet derivative of the matrix exponential [42], we readily get:

$$\begin{aligned} \dot{\mathbf{Q}} &= \frac{1}{\text{tr}[\exp(\mathbf{Y})]} \frac{d}{dt} \exp(\mathbf{Y}) - \exp(\mathbf{Y}) \frac{\text{tr}[\dot{\mathbf{Y}} \exp(\mathbf{Y})]}{\text{tr}[\exp(\mathbf{Y})]^2} \\ &= \frac{1}{\text{tr}[\exp(\mathbf{Y})]} \int_0^1 \exp((1-s)\mathbf{Y}) \dot{\mathbf{Y}} \exp(s\mathbf{Y}) ds - \mathbf{Q} \text{tr}[\mathbf{V}\mathbf{Q}] \\ &= \int_0^1 \mathbf{Q}^{1-s} \mathbf{V} \mathbf{Q}^s ds - \mathbf{Q} \text{tr}[\mathbf{V}\mathbf{Q}], \end{aligned} \quad (46)$$

and hence:

$$\begin{aligned} \mathbf{u}_\alpha^\dagger \dot{\mathbf{Q}} \mathbf{u}_\beta &= \int_0^1 \mathbf{u}_\alpha^\dagger \mathbf{Q}^{1-s} \mathbf{V} \mathbf{Q}^s \mathbf{u}_\beta ds - \text{tr}[\mathbf{V}\mathbf{Q}] \cdot \mathbf{u}_\alpha^\dagger \mathbf{Q} \mathbf{u}_\beta \\ &= \int_0^1 q_\alpha^{1-s} V_{\alpha\beta} q_\beta^s ds - q_\alpha \delta_{\alpha\beta} \sum_\gamma q_\gamma V_{\gamma\gamma}, \end{aligned} \quad (47)$$

where we have set $V_{\alpha\beta} = \mathbf{u}_\alpha^\dagger \mathbf{V} \mathbf{u}_\beta$. Thus, by carrying out the integration in (47), we finally obtain:

$$\mathbf{u}_\alpha^\dagger \dot{\mathbf{Q}} \mathbf{u}_\beta = \frac{q_\alpha - q_\beta}{\log q_\alpha - \log q_\beta} V_{\alpha\beta} - q_\alpha \delta_{\alpha\beta} \sum_\gamma q_\gamma V_{\gamma\gamma}, \quad (48)$$

with the convention $(x - y)/(\log x - \log y) = x$ if $x = y$. Eq. (23) then follows by substituting (48) in (45). \blacksquare

Proof of Proposition 1: Combining (MXL) and the derivative expression (46), we get:

$$\begin{aligned} \mathbf{Q}(n+1) &= \frac{\exp(\mathbf{Y}(n+1))}{\text{tr}[\exp(\mathbf{Y}(n+1))]} = \frac{\exp(\mathbf{Y}(n) + \gamma_n \mathbf{V}(n))}{\text{tr}[\exp(\mathbf{Y}(n) + \gamma_n \mathbf{V}(n))]} \\ &= \mathbf{Q}(n) + \gamma_n \int_0^1 \mathbf{Q}(n)^{1-s} \mathbf{V}(n) \mathbf{Q}(n)^s ds \\ &\quad - \gamma_n \text{tr}[\mathbf{Q}(n) \mathbf{V}(n)] \cdot \mathbf{Q}(n) + \mathcal{O}(\gamma_n^2 \|\mathbf{V}(n)\|^2), \end{aligned} \quad (49)$$

where the term $\mathcal{O}(\gamma_n \|\mathbf{V}(n)\|^2)$ is bounded from above by $C\gamma_n^2 \|\mathbf{V}(n)\|^2$ for some constant C that does not depend on $\mathbf{Q}(n)$. Since $\gamma_n \rightarrow 0$ by assumption, Remark 4.5 in [14] shows that the quadratic error in (49) can be ignored in the long-run, so $\mathbf{Q}(n)$ is an APT of the dynamics (46). Hence, by Proposition 3, the eigen-decomposition $\{q_\alpha(n), \mathbf{u}_\alpha(n)\}$ is an APT of (23), as claimed. \blacksquare

Proof of Theorem 3: Consider the following Euler discretization of the eigen-dynamics (23):

$$q_\alpha \leftarrow q_\alpha + \gamma_n q_\alpha \left(V_{\alpha\alpha} - \sum_\beta q_\beta V_{\beta\beta} \right), \quad (50a)$$

$$\mathbf{u}_\alpha \leftarrow \mathbf{u}_\alpha + \gamma_n \sum_{\beta \neq \alpha} \frac{V_{\beta\alpha}}{\log q_\alpha - \log q_\beta} \mathbf{u}_\beta, \quad (50b)$$

i.e. the update step of Alg. 3 without the orthonormalization correction for \mathbf{u}_α . We then obtain:

$$\mathbf{u}_\alpha^\dagger(n+1) \cdot \mathbf{u}_\beta(n+1) = \mathbf{u}_\alpha^\dagger(n) \cdot \mathbf{u}_\beta(n) + \mathcal{O}(\gamma_n^2), \quad (51)$$

which shows that the orthonormalization correction in Alg. 3 is quadratic in γ_n . Thus, as long as γ_n is chosen small enough (so that $q_\alpha(n) \geq 0$ for all n), Remark 4.5 in [14] shows that the iterates of Alg. 3 comprise an APT of (23). In turn, the same reasoning as in the proof of Prop. 1 can be used to show that $\mathbf{Q}(n) = \sum_\alpha q_\alpha(n) \mathbf{u}_\alpha(n) \mathbf{u}_\alpha^\dagger(n)$ is an APT of (MXL-c), so $\mathbf{Q}(n)$ converges to the solution set of (RM) by Theorem 1. ■

D. The fast-fading regime

Proof of Theorem 4: Let $\mathbf{V}_{\text{erg}} = \nabla R_{\text{erg}}$ denote the gradient of the ergodic sum rate function R_{erg} and consider the dynamics:

$$\begin{aligned} \dot{\mathbf{Y}} &= \mathbf{V}_{\text{erg}}, \\ \mathbf{Q} &= \frac{\exp(\mathbf{Y})}{\text{tr}[\exp(\mathbf{Y})]}. \end{aligned} \quad (52)$$

The same reasoning as in the proof of Theorem 5 shows that (52) converges to the unique minimizer of the (strictly concave) sum rate maximization problem (ERM). Moreover, given that R is concave for any fixed channel matrix \mathbf{H} and R_{erg} is finite on \mathcal{Q} , we have [43]:

$$\mathbf{V}_{\text{erg}} = \nabla_{\mathbf{Q}} R_{\text{erg}} = \mathbf{E}_{\mathbf{H}} [\nabla_{\mathbf{Q}} R(\mathbf{Q})] = \mathbf{E}_{\mathbf{H}}[\mathbf{V}], \quad (53)$$

with \mathbf{V} defined as in (11). With \mathbf{V} bounded, it follows that \mathbf{V}_{erg} is Lipschitz, so Propositions 4.2 and 4.1 in [14] imply that the iterates of (MXL) with noisy measurements satisfying (H1) and (H2) comprise a stochastic approximation of the mean dynamics (52). The rest of the proof then follows as in the case of Theorem 1. ■

REFERENCES

- [1] G. J. Foschini and M. J. Gans, "On limits of wireless communications in a fading environment when using multiple antennas," *Wireless Personal Communications*, vol. 6, pp. 311–335, 1998.
- [2] I. E. Telatar, "Capacity of multi-antenna Gaussian channels," *European Transactions on Telecommunications and Related Technologies*, vol. 10, no. 6, pp. 585–596, 1999.
- [3] J. Hoydis, S. ten Brink, and M. Debbah, "Massive MIMO in the UL/DL of cellular networks: How many antennas do we need?" *IEEE Trans. Wireless Commun.*, vol. 31, no. 2, pp. 160–171, February 2013.
- [4] F. Rusek, D. Persson, B. K. Lau, E. G. Larsson, T. L. Marzetta, O. Edfors, and F. Tufvesson, "Scaling up MIMO: Opportunities and challenges with very large arrays," *IEEE Signal Process. Mag.*, vol. 30, pp. 40–60, January 2013.
- [5] E. G. Larsson, O. Edfors, F. Tufvesson, and T. L. Marzetta, "Massive MIMO for next generation wireless systems," *IEEE Commun. Mag.*, vol. 52, no. 2, pp. 186–195, February 2014.
- [6] J. G. Andrews, S. Buzzi, W. Choi, S. Hanly, A. Lozano, A. C. K. Soong, and J. C. Zhang, "What will 5G be?" *IEEE J. Sel. Areas Commun.*, vol. 32, no. 6, pp. 1065–1082, June 2014.
- [7] R. S. Cheng and S. Verdú, "Gaussian multiaccess channels with ISI: capacity region and multiuser water-filling," *IEEE Trans. Inf. Theory*, vol. 39, no. 3, pp. 773–785, May 1993.
- [8] W. Yu, W. Rhee, S. Boyd, and J. M. Cioffi, "Iterative water-filling for Gaussian vector multiple-access channels," *IEEE Trans. Inf. Theory*, vol. 50, no. 1, pp. 145–152, 2004.
- [9] G. Scutari, D. P. Palomar, and S. Barbarossa, "Competitive design of multiuser MIMO systems based on game theory: a unified view," *IEEE J. Sel. Areas Commun.*, vol. 26, no. 7, pp. 1089–1103, September 2008.
- [10] T. L. Marzetta, "Noncooperative cellular wireless with unlimited numbers of base station antennas," *IEEE Trans. Wireless Commun.*, vol. 9, no. 11, pp. 3590–3600, 2010.
- [11] P. Mertikopoulos, E. V. Belmega, and A. L. Moustakas, "Matrix exponential learning: Distributed optimization in MIMO systems," in *ISIT '12: Proceedings of the 2012 IEEE International Symposium on Information Theory*, 2012, pp. 3028–3032.

- [12] P. Coucheney, B. Gaujal, and P. Mertikopoulos, "Distributed optimization in multi-user MIMO systems with imperfect and delayed information," in *ISIT '14: Proceedings of the 2014 IEEE International Symposium on Information Theory*, 2014.
- [13] P. Mertikopoulos, E. V. Belmega, A. L. Moustakas, and S. Lasaulce, "Distributed learning policies for power allocation in multiple access channels," *IEEE J. Sel. Areas Commun.*, vol. 30, no. 1, pp. 96–106, January 2012.
- [14] M. Benaïm, "Dynamics of stochastic approximation algorithms," in *Séminaire de Probabilités XXXIII*, ser. Lecture Notes in Mathematics, J. Azéma, M. Émery, M. Ledoux, and M. Yor, Eds. Springer Berlin Heidelberg, 1999, vol. 1709, pp. 1–68.
- [15] V. S. Borkar, *Stochastic Approximation: A Dynamical Systems Viewpoint*. Cambridge University Press and Hindustan Book Agency, 2008.
- [16] K. Tsuda, G. Rätsch, and M. K. Warmuth, "Matrix exponentiated gradient updates for on-line Bregman projection," *Journal of Machine Learning Research*, vol. 6, pp. 995–1018, 2005.
- [17] S. M. Kakade, S. Shalev-Shwartz, and A. Tewari, "Regularization techniques for learning with matrices," *The Journal of Machine Learning Research*, vol. 13, pp. 1865–1890, 2012.
- [18] P. Hall and C. C. Heyde, *Martingale Limit Theory and Its Application*, ser. Probability and Mathematical Statistics. New York: Academic Press, 1980.
- [19] V. H. de la Peña, "A general class of exponential inequalities for martingales and ratios," *The Annals of Probability*, vol. 27, no. 1, pp. 537–564, 1999.
- [20] P. Mertikopoulos and E. V. Belmega, "Transmit without regrets: online optimization in MIMO-OFDM cognitive radio systems," *IEEE J. Sel. Areas Commun.*, vol. 32, no. 11, pp. 1987–1999, November 2014.
- [21] T. Starr, J. M. Cioffi, and P. J. Silverman, *Understanding Digital Subscriber Line Technology*. Englewood Cliffs, NJ: Prentice Hall, 1999.
- [22] G. Scutari, D. P. Palomar, and S. Barbarossa, "The MIMO iterative waterfilling algorithm," *IEEE Trans. Signal Process.*, vol. 57, no. 5, pp. 1917–1935, May 2009.
- [23] —, "Simultaneous iterative water-filling for Gaussian frequency-selective interference channels," in *ISIT '06: Proceedings of the 2006 International Symposium on Information Theory*, 2006.
- [24] Y. Nesterov, "Primal-dual subgradient methods for convex problems," *Mathematical Programming*, vol. 120, no. 1, pp. 221–259, 2009.
- [25] A. M. Davie and A. J. Stothers, "Improved bound for complexity of matrix multiplication," *Proceedings of the Royal Society of Edinburgh, Section: A Mathematics*, vol. 143, no. 2, pp. 351–369, 4 2013.
- [26] A. S. Nemirovski, A. Juditsky, G. G. Lan, and A. Shapiro, "Robust stochastic approximation approach to stochastic programming," *SIAM Journal on Optimization*, vol. 19, no. 4, pp. 1574–1609, 2009.
- [27] T. W. Anderson, *An Introduction to Multivariate Statistical analysis*, 3rd ed. Wiley-Interscience, 2003.
- [28] A. J. Goldsmith and P. P. Varaiya, "Capacity of fading channels with channel side information," *IEEE Trans. Inf. Theory*, vol. 43, no. 6, pp. 1986–1992, 1997.
- [29] E. V. Belmega, S. Lasaulce, M. Debbah, and A. Hjørungnes, "Learning distributed power allocation policies in MIMO channels," in *EUSIPCO '10: Proceedings of the 2010 European Signal Processing Conference*, 2010.
- [30] M. Haenggi and R. K. Ganti, "Interference in large wireless networks," *Foundations and Trends in Networking*, vol. 3, no. 2, pp. 127–248, 2008.
- [31] L. E. Blume, "The statistical mechanics of strategic interaction," *Games and Economic Behavior*, vol. 5, pp. 387–424, 1993.
- [32] G. Calcev, D. Chizhik, B. Göransson, S. Howard, H. Huang, A. Kogiantis, A. F. Molisch, A. L. Moustakas, D. Reed, and H. Xu, "A wideband spatial channel model for system-wide simulations," *IEEE Trans. Veh. Technol.*, vol. 56, no. 2, p. 389, March 2007.
- [33] 3GPP, "User equipment (UE) radio transmission and reception," White paper, Jun. 2014.
- [34] A. Edelman, T. A. Arias, and S. T. Smith, "The geometry of algorithms with orthogonality constraints," *SIAM Journal on Matrix Analysis and Applications*, vol. 20, no. 2, pp. 303–353, 1998.
- [35] T. E. Abruđan, J. Eriksson, and V. Koivunen, "Steepest descent algorithms for optimization under unitary matrix constraint," *IEEE Trans. Signal Process.*, vol. 56, no. 3, pp. 1134–1147, March 2008.
- [36] V. Vedral, "The role of relative entropy in quantum information theory," *Reviews of Modern Physics*, vol. 74, no. 1, pp. 197–234, 2002.
- [37] R. T. Rockafellar, *Convex Analysis*. Princeton, NJ: Princeton University Press, 1970.
- [38] P. Mertikopoulos and W. H. Sandholm, "Regularized best responses and reinforcement learning in games," <http://arxiv.org/abs/1407.6267>, 2014.
- [39] J. Dattorro, *Convex Optimization & Euclidean Distance Geometry*. Palo Alto, CA, USA: Meboo Publishing, 2005.

- [40] G. H. Hardy, *Divergent Series*. Oxford University Press, 1949.
- [41] Y. S. Chow, "Convergence of sums of squares of martingale differences," *The Annals of Mathematical Statistics*, vol. 39, no. 1, 1968.
- [42] R. M. Wilcox, "Exponential operators and parameter differentiation in quantum physics," *Journal of Mathematical Physics*, vol. 8, no. 4, pp. 962–982, 1967.
- [43] V. Strassen, "The existence of probability measures with given marginals," *The Annals of Mathematical Statistics*, vol. 38, pp. 423–439, 1965.